Shape Optimization of H-beam Flange for Maximum Plastic Energy Dissipation[1]

P. Pan

JSPS Postdoctoral Fellow, Department of Architecture and Architectural Engineering, Kyoto University,
(Currently, Lecturer, Department of Civil Engineering, Tsinghua University, Beijing 100084, P.R. China)

M. Ohsaki

Department of Architecture and Architectural Engineering,
Kyoto University Kyotodaigaku-Katsura, Nishikyo, Kyoto 615-8540, Japan

H. Tagawa

Department of Environmental Engineering and Architecture, Nagoya University,
Furo-cho, Chikusa, Nagoya 464-8603, Japan

Abstract

The purpose of this paper is to show that the performance of a structural component is drastically improved utilizing shape optimization considering inelastic responses. Optimal flange shapes are found as an example for an H-beam to show that the the energy dissipation capacity is significantly improved by shape optimization. The forced displacement is given at the free end of the cantilever beam so that the average deformation angle reaches the specified value. The constraint is given for the maximum equivalent plastic strain at the welded section. Global optimal solutions are searched by a heuristic approach called simulated annealing, which is successfully combined with a commercial finite element analysis code ABAQUS for elastoplastic analysis. It is shown in the examples that the maximum plastic strains near the welded section are reduced and the plastic deformation is widely distributed around the reduced section of the optimal solution; thus, allowing large energy dissipation under small maximum plastic strain. The results show the advantage of the optimal shape over the conventional circular cut.

Keywords Optimization; Beam; Flanges; Energy dissipation; Algorithms

[1]This paper has appeared in: J. Struct. Eng., ASCE, Vol. 133(8), pp. 1176–1179, 2007.

1 Introduction

Recent rapid developments of computational technologies and optimization algorithms enabled us to optimize real-world structures under constraints that are required in design practice. In addition to optimizing structural systems, it is possible to find optimal shapes of structural components or parts discretized to finite elements; e.g. shapes of automobile suspensions, airfoil wings, and so on (Bendsøe and Sigmund, 2003). In the civil engineering field, however, optimization of structural components has not been well investigated.

The 1994 Northridge earthquake caused widespread damage to steel moment-resisting frames mainly due to brittle fracture near the beam-to-column flange groove welds. In response to such damage, the Reduced Beam Section (RBS) connection has been extensively investigated (Chen *et al.*, 1996; Iwankiw and Carter, 1996; Goel *et al.*, 1997; Engelhardt, 1999). In an RBS moment connection, a portion of the beam flange is selectively trimmed in the region adjacent to the beam-to-column connection in order to force the plastic hinge to be located within the reduced section, and thereby reducing the possibility of fracture occurring at the beam-to-column flange groove weld and the surrounding base metal. Various shapes of cutouts have been investigated, including a constant cut, a tapered cut and a circular cut (Engelhardt *et al.*, 2000). However, only an optimization based on predetermined cutout shapes has been presented (Jones *et al.*, 2002), and no systematic process for finding the optimal shape has been found.

Optimization of elastoplastic structures has been extensively investigated during the 1990s, including sensitivity analysis of path-dependent problems (Ohsaki and Arora, 1994; Ohsaki, 1997; Swan and Kosaka, 1997). However, analytical evaluation of sensitivity coefficients requires substantial computational cost. Heuristic approaches have been developed to obtain approximate optimal solutions within reasonable computational time, although there is no theoretical proof of convergence. Simulated Annealing (SA) (Aarts and Korst, 1989) is used in this study to search for a global optimal solution without evaluation of sensitivity coefficients. SA has been successfully applied to many structural optimization problems (Balling, 1991; Tagawa and Ohsaki, 1999), and is applicable to both problems with continuous and discrete variables.

The main purposes of this paper is summarized as follows:

- The performance of a structural component is shown to be drastically improved utilizing shape optimization considering inelastic responses.
- A commercial finite element analysis program can be successfully combined with the optimization algorithm with SA.
- As an example, shapes of beam flanges are optimized to maximize the dissipated energy for forced displacement against static load with the constraint on the maximum equivalent plastic strain along the welded section at the beam-to-column connection.

2 Optimization problem and optimization algorithm

Consider a cantilever beam that represents half of a beam in a frame. One end is fixed and the other end is free to simulate the inflection point at the mid-span of the beam. Optimal flange shapes are to be found for a beam subjected to a static loading condition defined by forced displacement at the free end.

The beam is discretized into finite elements. The shape of the flange is defined by a cubic spline curve, and the design variables are the locations of the control points. Let $\mathbf{x}$ denote the vector consisting of the variable coordinates of the control points. The upper and lower bounds for $\mathbf{x}$ are denoted by $\mathbf{x}^{\mathrm{U}}$ and $\mathbf{x}^{\mathrm{L}}$, respectively. A component of a vector is indicated by a subscript; i.e., $\mathbf{x} = \{x_i\}$.

The objective function is the dissipated energy throughout the loading history, which is denoted by $E(\mathbf{x})$ as a function of $\mathbf{x}$. Since the final deformed state is defined by the specified displacement, unfavorable local plastification can be avoided by maximizing $E(\mathbf{x})$. The upper bound $\bar{\varepsilon}^{\mathrm{p}}$ is given for the maximum equivalent plastic strain ε^{p} among the elements at the fixed end to prevent fracture at the beam-to-column flange groove welds. Hence, the optimization problem is formulated as

$$\text{maximize} \quad E(\mathbf{x}) \tag{1}$$

$$\text{subject to} \quad \varepsilon^{\mathrm{p}}(\mathbf{x}) \leq \bar{\varepsilon}^{\mathrm{p}} \tag{2}$$

$$x_i^{\mathrm{L}} \leq x_i \leq x_i^{\mathrm{U}}, \quad (i = 1, \dots, m) \tag{3}$$

where m is the number of design variables.

Since the optimization problem stated above is highly nonlinear, it is solved by SA which is categorized as a statistical heuristic search. Since the algorithm needs very few problem dependent parameters, it is quite robust even for an objective function that has many local optima. Note that other methods such as random start nonlinear programming with the finite difference method for gradient computation (Pan *et al.*, 2007) and approximation using response surface (Ogawa *et al.*, 2005) can also be used. However, the purpose of this paper is not to present an optimization method, but to show that shape optimization can be effectively applied to improve the elastoplastic performance of the structural parts.

We use the SA for continuous variables by Goffe *et al.* (1994). The main feature of this method is that it controls the size of the most promising region by the maximum distance to the neighborhood solutions, which is initially moderately large and gradually adjusted to an appropriate value. The constraint $\varepsilon^{\mathrm{p}} \leq \bar{\varepsilon}^{\mathrm{p}}$ is incorporated by a penalty function approach using the penalty parameter η as

$$\tilde{E}(\mathbf{x}) = E(\mathbf{x}) - \eta \max(0, \varepsilon^{\mathrm{p}}(\mathbf{x})/\bar{\varepsilon}^{\mathrm{p}} - 1) \tag{4}$$

The algorithm depends on the following parameters: number of function evaluations before reducing the size of the neighborhood is defined by mN_{S}; number of function evaluations before reducing the temperature is defined by $mN_{\mathrm{S}}N_{\mathrm{T}}$; the objective function is scaled by $1/c$; initial temperature and its reduction ratio is given by T and μ, respectively; the average initial solution and the initial size of the most promising region for x_i are defined by $\bar{x}_i$ and d_i, respectively. See Goffe *et al.* (1994) for the details.

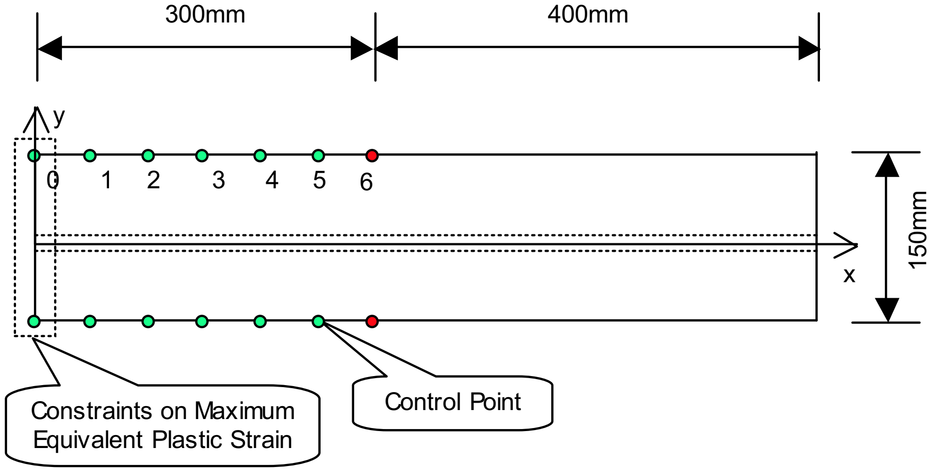

Fig. 1: Normal flange shape.

3 Optimization results

Optimal flange shapes are found for a wide-flange cantilever beam with length 700 mm and a cross-section of $\mathrm{H} - 150 \times 150 \times 7 \times 10$; i.e., the span-height ratio is $700 \times 2/150 = 9.33$.

The normal flange shape is shown in Fig. 1. The flange width is to be varied at the 300 mm region from the welded section (fixed end). The control points for the cubic spline curve are also given in Fig. 1. The location of the control point 6 is fixed, and the points 0–5 can move only in y-direction. Hence, the number of design variables (y-coordinates) is 6 considering the symmetry condition with respect to the x-axis. Only reduction is allowed for the flange width at the control point, and the upper and lower bounds of the variables are 75.0 mm and 25.0 mm, respectively.

Optimization is to be carried out to maximize the dissipated energy E under monotonic loading condition up to the displacement 14 mm at the free end, which corresponds to average rotation angle $\theta = 0.02$. The upper-bound constraint is given for the maximum equivalent plastic strain ε^{p} among the elements along the fixed end.

The parameters for SA are $N_{\mathrm{T}} = 2$, $N_{\mathrm{S}} = 20$, $c = 100$, $T = 1.0$. The penalty parameter is set as $\eta = 0.85$ so that the magnitude of the penalty term in (4) is about 10-times as large as the possible value of E at the initial temperature. The initial values are specified as $\bar{x}_i = 75.0$, $d_i = 10.0$. The process is terminated if the improvement of $\tilde{E}$ is less than the small value 0.1 within consecutive four steps of decreasing the temperature.

Geometrically nonlinear elastoplastic analysis is carried out by ABAQUS Ver. 6.5.1 (ABAQUS, 2004), which is a general purpose finite element code. S4R, which is a 4-node quadrilateral thick shell element with reduced integration and a large-strain formulation, is used for modeling. A coarse mesh is used for optimization and its accuracy is investigated by analysis with a fine mesh. The total numbers of elements and freedom of displacement for the coarse mesh are 504 and 3306, respectively. The

Table 1: Dissipated energy E and maximum plastic equivalent strain ε^{p} at the fixed end.

	Optimal shape (Coarse mesh)		Verification (Fine mesh)	
	E	ε^{p} ($\times 10^{-3}$)	E	ε^{p} ($\times 10^{-3}$)
Case 0	950	17.2	949	29.35
Case 1	875	1.00	871	1.12
Case 2	893	2.00	891	3.65
Case 3	900	4.00	899	6.42
Case 4	912	7.95	908	11.27

elastic modulus is 2.05×10^5 N/mm^2 and Poisson's ratio is 0.3. The yield stress is 235.0 N/mm^2 and the hardening ratio is 0.001. The J_2 associated flow theory and linear kinematic hardening with Ziegler's rule are adopted.

The ABAQUS analysis is iteratively called from the SA algorithm. SA program generates new coordinates of the control points, which are transmitted to ABAQUS preprocessing module controlled by Python script language (David, 2001), that creates the beam model and submits a job through '.inp' file to ABAQUS/standard analysis. The analysis results are stored in '.odb' file. A postprocessing module also written in Python script language is used to extract the necessary data such as E and ε^{p}, which are called ALLPD and PEEQ in ABAQUS. The data are returned to the SA program for the new round of iteration. A PC with Intel Xeon 3.4 GHz CPU and 2GB RAM is used for the computation.

Optimal shapes are found under monotonic loading condition and the results are compared with those of the normal beam with uniform flange width (Case 0). Optimal shapes and their distribution of ε^{p} for Cases 1–4 corresponding to $\bar{\varepsilon}^{\mathrm{p}} = 0.001$, 0.002, 0.004, and 0.008, respectively, are shown in Figs. 2(a)–(d), where darker color represents larger values. The result of Case 0 is also shown in Fig. 2(e).

Basically, the optimal shapes share a similar pattern featured with a single concave region, which has two functions: (1) shift the maximum deformation demand from the fixed end to the middle sections, and (2) increase the plastification area for the specified average rotation angle θ. The distribution of ε^{p} shows that its maximum value exists at the fixed end for Case 0, whereas it is successfully shifted to the concave region for Cases 1–4. It should also be noted that plastification region of Cases 1–4 are longer than that of Case 0. Therefore, the total plastified areas of the optimized flange are not much smaller than that of Case 0, although the concavity decreases the flange width of the plastified region.

The optimal solution is found within 6000 analyses for each case. The total number of analysis is 11761 for Case 1, and the elapsed time for optimization is 63.06 hours (20 sec. per analysis). However, only 15% is used for analysis, and remaining portion of the time is; 5% for preprocess, 5% for postprocess, 75% for ABAQUS license checking, and the time used for SA algorithm is negligible.

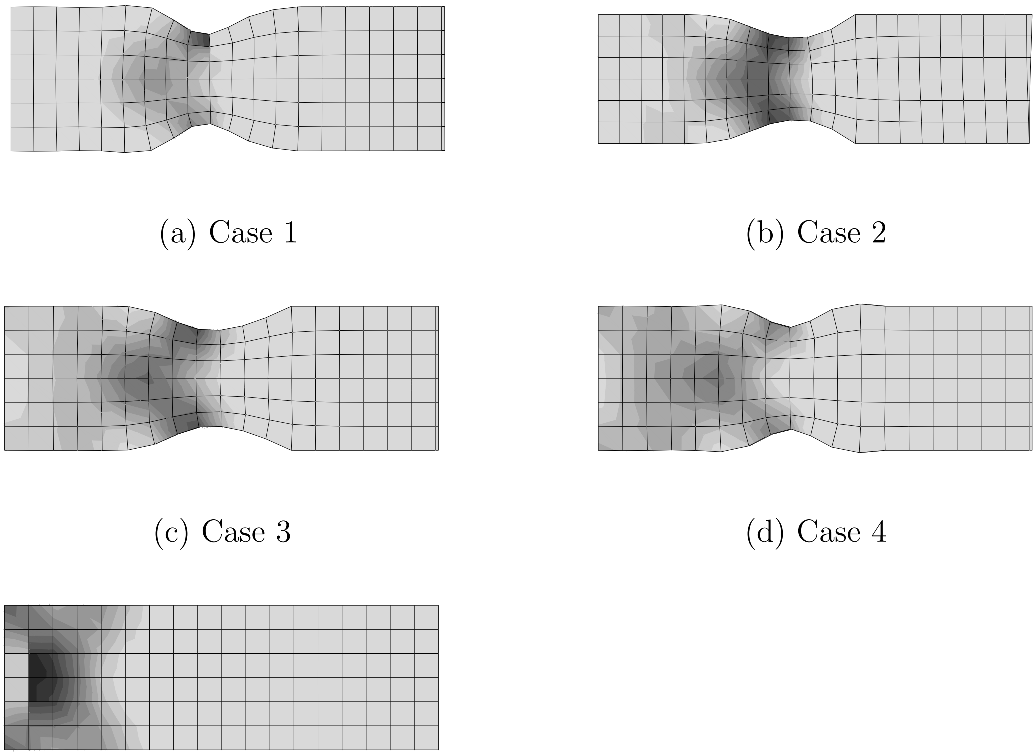

(a) Case 1

(b) Case 2

(c) Case 3

(d) Case 4

(e) Case 0

Fig. 2: Distribution of equivalent plastic strain of the normal and optimal beams.

Note from Fig. 2 that the flange shapes strongly depend on the value of $\bar{\varepsilon}^{\mathrm{p}}$. Obviously, larger reduction of the width is needed for smaller value of $\bar{\varepsilon}^{\mathrm{p}}$ to suppress the deformation at the welded section for the specified θ. The value of $\bar{\varepsilon}^{\mathrm{p}}$ in practice can be defined by the design criteria along with the concept of the performance-based design.

The dissipated energy E and ε^{p} at the fixed end of Cases 1–4 with coarse mesh, as well as Case 0, are shown in Table 1 for the final deformed state. It is seen from Table 1 that E decreases with the decrease of $\bar{\varepsilon}^{\mathrm{p}}$, because the objective function is smaller for a stricter constraint in a maximization problem. It is seen that E of Case 0 is not much different from those of Cases 1–4, whereas ε^{p} of Case 0 is significantly larger compared with those of Cases 1–4. For instance, almost the same (with a difference less than 5%) dissipated energy of Case 0 is achieved by Case 4 with less than half value of ε^{p} (7.95×10^{-3} for Case 4 and 17.2×10^{-3} for Case 0).

To further demonstrate the effect of flange shape optimization, E and θ of Case 0 for specified $\bar{\varepsilon}^{\mathrm{p}}$ are computed; i.e., the analysis for Case 0 is terminated at each specified value of $\varepsilon^{\mathrm{p}} = \bar{\varepsilon}^{\mathrm{p}}$ The values of (E, θ) for $\bar{\varepsilon}^{\mathrm{p}} = 0.001$, 0.002, 0.004 and 0.008 are (36, 0.006), (84, 0.007), (188, 0.008) and (404, 0.012), respectively; i.e., the value of E of

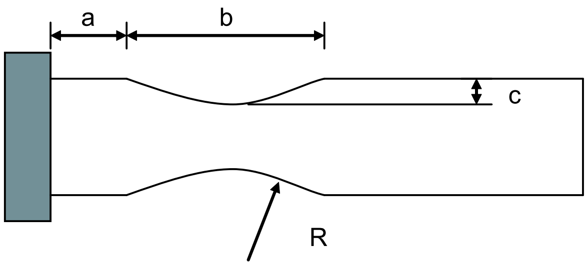

Fig. 3: Definition of circular cut.

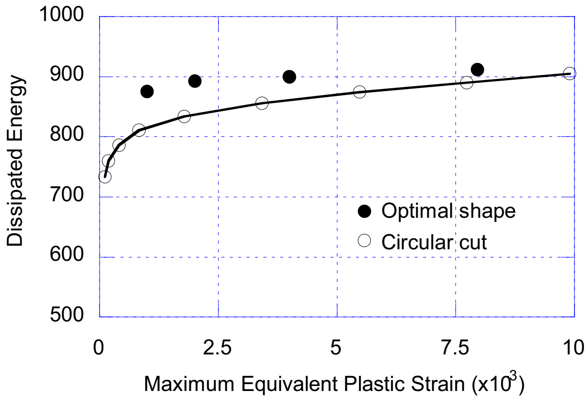

Fig. 4: Comparison of E and ε^{p} between circular cut and optimal shape.

normal beams are far smaller than those of the optimal beams for the same value of $\bar{\varepsilon}^{\mathrm{p}}$. Hence, the energy dissipation capacity is drastically improved by optimization. The resulting value of θ of the normal beam for $\bar{\varepsilon}^{\mathrm{p}} = 0.001, 0.002, 0.004$ and 0.008 are 0.006, 0.007, 0.008 and 0.012, respectively, which are all significantly smaller than 0.02 for the optimal solutions. Therefore, the beam with optimal flange shape can avoid large equivalent plastic strain at the welded section to improve its deformation capacity.

To investigate the mesh convergence, results by a fine mesh with double density in each direction are shown in Table 1. It is found that the coarse mesh accurately predicts E, but not enough to predict ε^{p} because of the stress concentration at the corner of the fixed end. This singularity occurs due to the unrealistic idealizations used in the finite element model; i.e., the welded section is completely fixed although in reality it deforms with the panel at the connection. If the exact stress and strain at the connection is required, more detailed modeling is needed. However, the analysis of the detailed modeling is too expensive for optimization. Therefore, the coarse mesh has been used.

The performances of the optimal shape are compared with those of the conventional RBS shape of circular cut, where the parameters are defined in Fig. 3. The values of a and b are fixed at 75 mm and 200 mm, respectively, and c (mm) is varied as $17.5, 20.0, \ldots, 37.5$. It is seen from Fig. 4 that larger energy can be dissipated by the optimal shapes than circular cut for the same value of ε^{p}.

4 Conclusions

Optimal flange shapes have been found for a cantilever H-beam subjected to static loads. The objective function to be maximized is the plastic dissipated energy. The constraint is given for the maximum equivalent plastic strain at the welded section (fixed end) under the specified forced displacement at the free end. The conclusions drawn from this study are summarized as

1. The energy dissipation capacity can be improved by optimizing the flange shape.
2. Optimal shapes can be successfully obtained by SA in conjunction with a commercial finite element analysis code.
3. The optimal shape strongly depends on the upper bound of the equivalent plastic strain, which is to be specified in practice based on the performance required for each frame.

Although the computational cost for optimization is very large, the results of this study ensures that the performances of the structural parts can be effectively improved by shape optimization.

5 Acknowledgement

Financial support by the Ministry of Education, Culture, Sports, Sciences and Technology of Japan under Grant No. 17360270 and No. 16-4364 is gratefully acknowledged.

References

Aarts, E. and Korst, J. (1989). *Simulated Annealing and Boltzmann Machines: A Stochastic Approach to Combinatorial Optimization and Neural Computing.* Wiley, Chichester, England.

ABAQUS (2004). *ABAQUS version 6.4 documentation.* ABAQUS, Inc.

Balling, R. J. (1991). Optimal steel frame design by simulated annealing. *J. Struct. Engng., ASCE*, **117**(6), 1780–1795.

Bendsøe, M. P. and Sigmund, O. (2003). *Topology Optimization: Theory, Methods and Applications.* Springer.

Chen, S. J., Yeh, C. H., and Chu, J. M. (1996). Ductile steel beam-to-column connections for seismic resistance. *J. Struct. Engng., ASCE*, **122**(11), 1292–1299.

David, B. (2001). *Python Essential Reference (2nd Edition).* New Riders Publishing.

Engelhardt, M. D. (1999). The 1999 t. r. higgins lecture: Design of reduced beam section moment connections. In *Proc., 1999 North American Steel Construction Conf., Tront*, pages 1–29.

Engelhardt, M. D., Fray, G. T., S. Jones, M. V., and Holliday, S. (2000). Behavior and design of radius cut, reduced beam section connections. Technical report, SAC Joint Venture, Sacramento, Calif.

Goel, S. C., Stojadinovic, B., and Lee, K. H. (1997). Truss analogy for steel moment connections. *Eng. J.*, **37**(2), 43–53.

Goffe, W. L., Ferrier, G. D., and Rogers, J. (1994). Global optimization of statistical functions with simulated annealing. *J. ournal of Econometrics*, **60**(1), 65–99.

Iwankiw, N. R. and Carter, C. (1996). The dogbone: a new idea to chew on. *Modern Steel Constr.*, **36**(4), 18–23.

Jones, S. L., Fry, G. T., and Engelhardt, M. D. (2002). Experimental evaluation of cyclically loaded reduced beam section moment connections. *J. Struct. Eng.*, **128**(4), 441–451.

Ogawa, T., Ohsaki, M., Miyamura, T., and Kumagai, T. (2005). Shape optimization of shell roofs subjected to strong wind by using a variable complexity model. *J. Int. Assoc. for Shell and Spatial Struct.*, **46**(2), 110–115.

Ohsaki, M. (1997). Sensitivity analysis of elastoplastic structures by using explicit integration method. *Appl. Mech. Rev.*, **50**(11), 156–161.

Ohsaki, M. and Arora, J. S. (1994). Design sensitivity analysis of elasto-plastic structures. *Int. J. Num. Meth. Engng.*, **37**, 737–762.

Pan, P., Ohsaki, M., and Kinoshita, T. (2007). Constraint approach to performance-based design of steel moment-resisting frames. *Engineering Structure*, page Published online.

Swan, C. C. and Kosaka, I. (1997). Voigt–reuss topology optimization for structures with nonlinear material behaviors. **40**, 3785–3814.

Tagawa, H. and Ohsaki, M. (1999). A continuous topology transition model for shape optimization of plane trusses with uniform cross-sectional area. In *Proc. 3rd World Congress of Structural and Multidisciplinary Optimization (WCSMO3)*.